Scientific Research Publishing

Open Journal of Radiology, 2024, 14, 14-23
https://www.scirp.org/journal/ojrad
ISSN Online: 2164-3032
ISSN Print: 2164-3024

Anisotropy of Trabecular Bone from Ultra-Distal Radius Digital X-Ray Imaging: Effects on Bone Mineral Density and Age

Jian-Feng Chen

Department of Radiology and Medical Imaging, Stritch School of Medicine, Loyola University Medical Center, Chicago, USA
Email: jfchen@live.com

How to cite this paper: Chen, J.-F. (2024) Anisotropy of Trabecular Bone from Ultra-Distal Radius Digital X-Ray Imaging: Effects on Bone Mineral Density and Age. *Open Journal of Radiology*, **14**, 14-23.
https://doi.org/10.4236/ojrad.2024.141002

Received: February 18, 2024
Accepted: March 16, 2024
Published: March 19, 2024

Abstract

Background: When applied to trabecular bone X-ray images, the anisotropic properties of trabeculae located at ultra-distal radius were investigated by using the trabecular bone scores (*TBS*) calculated along directions parallel and perpendicular to the forearm. **Methodology:** Data from more than two hundred subjects were studied retrospectively. A DXA (GE Lunar Prodigy) scan of the forearm was performed on each subject to measure the bone mineral density (*BMD*) value at the location of ultra-distal radius, and an X-ray digital image of the same forearm was taken on the same day. The values of trabecular bone score along the direction perpendicular to the forearm, TBS_x, and along the direction parallel to the forearm, TBS_y, were calculated respectively. The statistics of TBS_x and TBS_y were calculated, and the anisotropy of the trabecular bone, which was defined as the ratio of TBS_y to TBS_x and changed with subjects' *BMD* and age, was reported and analyzed. **Results:** The results show that the correlation coefficient between TBS_x and TBS_y was 0.72 ($p < 0.001$). Trabecular bone anisotropy changed with subjects' *BMD* and age was reported. The results showed that decreased trabecular bone anisotropy was associated with deceased *BMD* and increased age in the subject group. **Conclusions:** This study shows that decreased trabecular bone anisotropy was associated with decreased *BMD* and increased age.

Keywords

Anisotropy, Trabecular Bone Score, Bone Mineral Density, Ultra-Distal Radius, Digital X-Ray Image

1. Introduction

Osteoporosis is a bone disease characterized by low bone mineral density (*BMD*)

and micro-architectural deterioration of bone tissue [1]. The *BMD* measurement by using dual energy X-ray absorptiometry (DXA) is defined by the World Health Organization (WHO) Working Group as the gold standard and is clinically used to diagnose osteoporosis [2]. *BMD* is clearly one of the major determinants of bone strength and fracture risk [3] [4] [5], but the assessment of fracture risk by *BMD* sometime may still lack enough sensitivity [6]. It is clear that other factors in addition to *BMD* may account for bone strength and fracture risk. They could include bone micro-architecture, bone geometry, and other extra-skeletal factors [6]. The trabecular structure with specific reference to bone micro-architecture, known to affect bone fragility, may not be completely accounted for by standard DXA measurements, but alternative approaches, such as Trabecular Bone Score (*TBS*), have been proposed in order to overcome this limitation [6] [7] [8]. *TBS* originally was defined as the slope at the origin of the log-log representation of 2D projected image evaluated from least square regression line calculation, and is a novel texture parameter that evaluated pixel gray-level local variations in a DXA lumbar spine or human femur image and may directly related to bone micro-architecture and fragility fracture risk [6], and might improve the prediction accuracy for major osteoporotic fractures in elderly people [8]. Conceptually, a dense trabecular network, associated with strong mechanical bone strength, produces a projection image with many fine gray-level texture variations of small amplitude and therefore a steep slope. In contrast, a loose trabecular network, associated with weak mechanical bone strength, produces a projection image with fewer fine gray-level texture variations of large amplitude and therefore a shallow slop. Furthermore, mechanical and structural properties of trabecular bone are anisotropic rather than isotropic in general [9] [10], which has been observed through variation of the mechanical behavior of trabecular bone following specific testing directions. The anisotropy of trabecular bone corresponds to these variations and may be considered to predict the fracture risk. In our previous paper [11], we only studied the initial Slope of variogram of digital X-Ray images along the direction of perpendicular to the forearm. In the current study, first, the values of trabecular bone score along the direction of perpendicular to the forearm, TBS_x, and along the direction of parallel to the forearm, TBS_y, were calculated respectively. The statistics of TBS_x and TBS_y were calculated and analyzed. The ratio of TBS_y/TBS_x was used to study the trabecular bone anisotropy. If the ratio deviates from one, trabecular bone will demonstrate greater anisotropy; otherwise, if the ratio is closer to one, it will demonstrate greater isotropy. This anisotropy changed with subjects' *BMD* and age will be reported.

2. Materials and Methods

Study Subjects

In order to study the properties of TBS_x and TBS_y of trabecular bone located at ultra-distal radius, both radiographic and *BMD* data from a group of 98 male

and 128 female adults, who were recruited and participated in the project of *BMD* measurements and osteoporosis assessments with radiographer at two hospitals in China, were studied retrospectively [11]. The participants were originally screened by detailed questionnaire, disease history, and physical examination. Their ages ranged from 23 to 87 years old, with an average age of 62 years. Participants were excluded if they had a history of forearm trauma and cancer.

A typical digital X-ray image of the ultra-distal radius, as shown in **Figure 1**, was obtained by using a commercial available digital radiographic system. These digital X-ray images could qualitatively show the image texture difference between normal and abnormal bones due to deteriorate microarchitecture of bone. As a typical setup for X-ray imaging of extremities, the acquisition parameters for these digital X-ray images were set as 55 *kVp* and 10 *mAs* (100 *mA* and 100 *msec*) with a specific SID (source-to-image distance) of 100 cm, and a X-ray focal spot of 0.6 mm. No any added X-ray filtration was used. According to the detector specifications, the digital image detector has 3 $k \times 3$ k pixels matrix with a pixel size of 0.139 mm, and the image signal has a gray level depth of 12 bits. In order to reduce Heel effect of X-ray imaging, the region of interest (ROI) was put in the center of X-ray beam (around the original point of X-ray image).

Calculation of the Trabecular Bone Scores TBS_x and TBS_y

In our study, a digital 2D X-ray image signal, $I(i, j)$, was used for both TBS_x and TBS_y calculation, where (i, j) were the spatial coordinates. First, the experimental variogram $V_x(k)$ vs k is calculated by averaging the squared differences of the image signal values at several pairs of points with a specified separation, k, along the direction perpendicular to the forearm, as shown in **Figure 2(a)**:

$$V_x(k) = \frac{1}{2M \times N} \sum_{i=1}^{M} \sum_{j=1}^{N} \left[I(i, j) - I(i+k, j) \right]^2 \quad (1)$$

Figure 1. Representative image depicting the ultra-distal radius of subjects obtained using a digital X-ray imaging system.

where $M \times N$ is the total number of data pairs $I(i, j)$ and $I(i+k, j)$ within the region of interest (ROI). ROI starts at the bifurcation of the radius and ulna, and the coverage range is 1/12 length of radius, and is similar to the ROI of ultra-distal radius defined for GE Prodigy, and has an enclosed area within ultra-distal radius [12], as shown in **Figure 2(b)**. Similarly, the experimental variogram $V_y(k)$ vs k is calculated by averaging the squared differences of image signal values at several pairs of points with a specified separation, k, along the direction of parallel to the forearm, as shown in **Figure 2(a)**:

$$V_y(k) = \frac{1}{2M \times N} \sum_{i=1}^{M} \sum_{j=1}^{N} \left[I(i, j) - I(i, j+k) \right]^2 . \quad (2)$$

Then, the values of trabecular bone scores, TBS_x and TBS_y, were calculated from the slopes at the origin of log-log representation of $V_x(k)$ and $V_y(k)$, evaluated from the slope of least-square regression line (by using a line of best fit) calculation over the four points of $k = 1$, 2, 3, and 4, or $\log_{10}(k) = 0$, 0.301, 0.477, and 0.602, as shown in **Figure 3**.

BMD Measurements with DXA

The measurement of *BMD* at ultra-distal radius was performed for all participants using a GE Lunar Prodigy DXA scanner (GE Healthcare, Madison, WI) running enCORE software version 13.31, which is designed to make DXA even more powerful [12]. During the study, the DXA scanner was calibrated with a GE Lunar aluminum spine phantom to avoid any affect from significant drift and/or shift on our study. For *BMD* measurements, each subject was asked to sit beside the scanning table in a chair without any arms or wheels. The subject was asked to keep the forearm immobile during scanning and the forearm was scanned parallel to the long axis of the table. The scanning range was from the center of wrist to the proximal forearm according to the operation manual provided by the manufacturer.

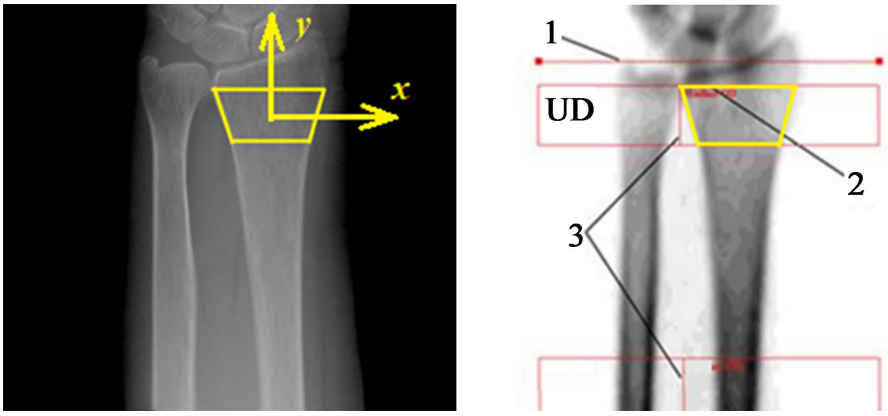

Figure 2. ROI used for our analysis starts from the reference point of the bifurcation of the radius and ulna, and the coverage range is 1/12 length of radius as shown in (a), and is similar to the ROI of ultra-distal radius area defined for GE Prodigy as shown in (b) [11]. Here *x*-axis is in the direction of perpendicular to the forearm, and *y*-axis is in the direction of parallel to the forearm.

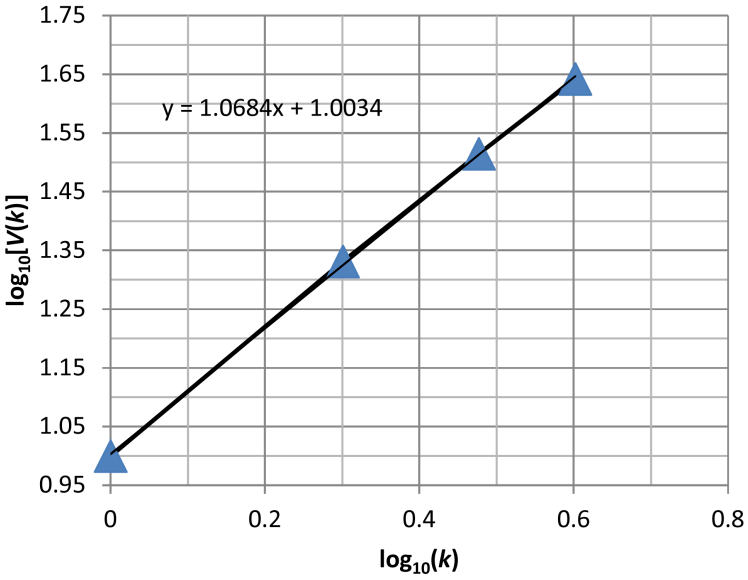

Figure 3. The calculation of TBS_x and TBS_y of and as the slopes at the origin of the experimental variogram, where k is the separation (in pixels) between a pair of imaging position.

Statistical Analysis

Pearson correlation coefficients for TBS_x and TBS_y of trabecular bone located at ultra-distal radius were calculated. Person correlation coefficient is given by [13].

$$\rho = \frac{\sum_{i=1}^{N_1}\left(X_i - \bar{X}\right)\left(Y_i - \bar{Y}\right)}{\sqrt{\sum_{i=1}^{N_1}\left(X_i - \bar{X}\right)^2 \sum_{i=1}^{N_1}\left(Y_i - \bar{Y}\right)^2}} \tag{3}$$

where ρ is the Pearson correlation coefficient, X_i is the TBS_x, and Y_i is the TBS_y for the subject i. $\bar{X}$ is the mean of $\overline{TBS_x}$, $\bar{Y}$ is the mean of $\overline{TBS_y}$, and N_1 is the total number of subjects. Then, both linear regressions and their R-squared values are also calculated. Here R-squared value shows how well the data fit the regression model.

3. Results

Participant Characteristics

Among 228 subjects, 43% were men (98/228) with an average age 57.7 ± 19.5 years, and 57% were women (130/228) with an average age 65.3 ± 13.3 years. The BMD of ultra-distal radius was 0.522 ± 0.088 g/cm^2 for men, and 0.350 ± 0.103 g/cm^2 for women. The average TBS_x of ultra-distal radius was 1.081 ± 0.096 cm^{-1} in both men and women. The average TBS_y of ultra-distal radius was 1.184 ± 0.071 cm^{-1} in men, and 1.163 ± 0.069 cm^{-1} in both men and women. The Pearson correlation coefficient between TBS_x and TBS_y for the trabecular bone located at ultra-distal radius is 0.72 ($p < 0.001$), as shown in **Figure 4**. The ratio of TBS_y/TBS_x has a slight positive correlation with the subject's *BMD*, as shown in **Figure 5**, and a slight negative correlation with the subject's age, as shown in **Figure 6**, and will approach to 1, when subject's age increases, as shown in **Figure 6**. These

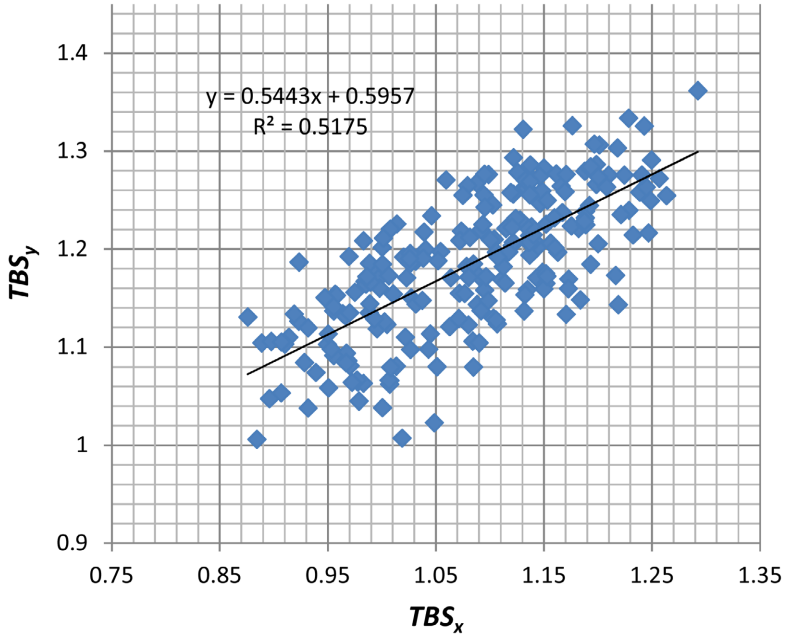

Figure 4. The correlation coefficient between TBS_x and TBS_y of trabecular bone located at ultra-distal radius, and linear regression lines with R-squared value = 0.52.

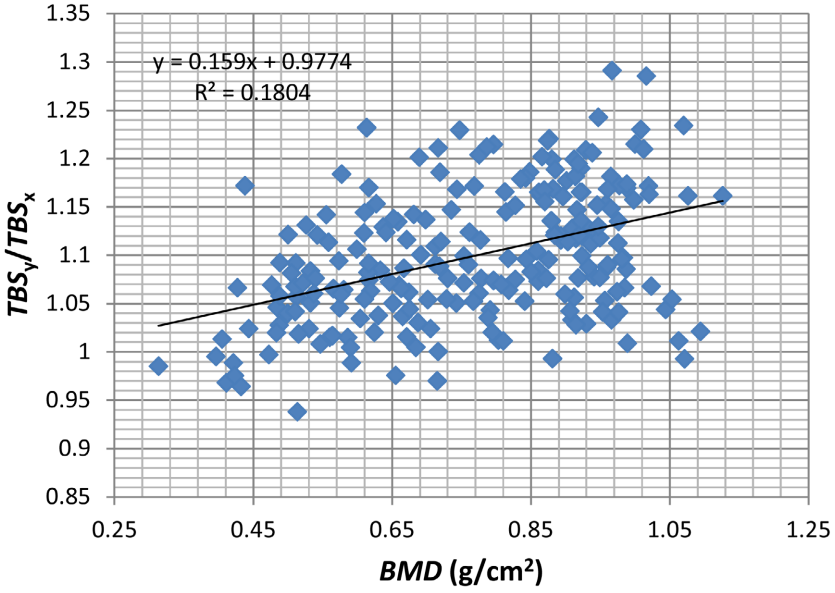

Figure 5. The ratio of TBS_y/ TBS_x as a function of subjects' *BMD*.

results suggest that healthier trabecular bone located at the ultra-distal radius will have greater anisotropy.

4. Discussion

Osteoporosis is defined as a systemic skeletal disease characterized by low bone mass density and micro-architectural degradation of bone tissue, with an increase in bone fragility to fracture. Current study shows that a decrease in *BMD* could often be accompanied by bone micro-architectural deterioration. Pothuaud

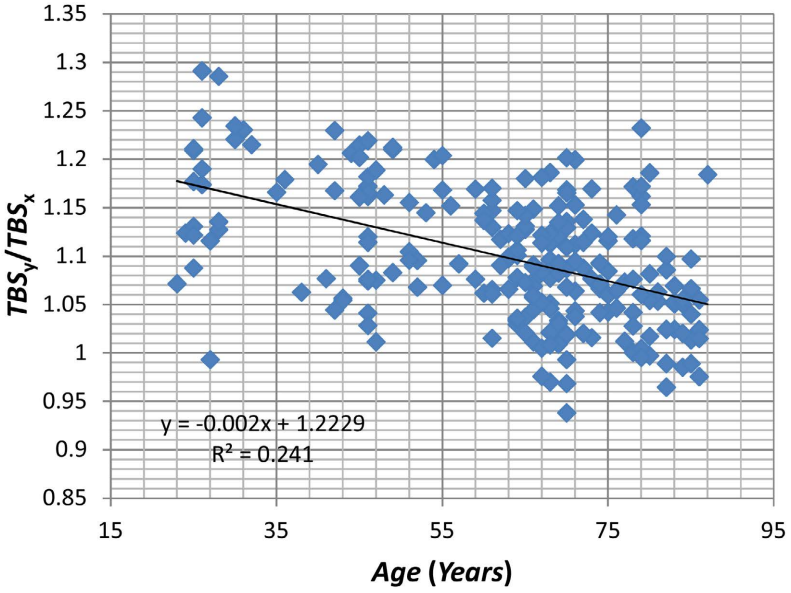

Figure 6. The ratio of TBS_y/TBS_x as a function of subjects' age.

et al. introduced a parameter called trabecular bone score (*TBS*) which is a texture index that evaluates pixel gray-level variations of 2D projection images of the trabecular bone from human lumbar spines acquired by DXA scanners [6], providing an indirect index of trabecular architecture. *TBS* is defined as the initial slope of the log-log transform of variogram, which describes the rate of changes of variance with respect to a lag distance. Significant correlations were observed between *TBS* and microarchitecture parameters (e.g. bone volume fraction and trabecular number) of trabecular bone from human femurs and lumbar spines [6]. A dense trabecular structure produces a 2D image with a large number of pixel value variations of small amplitude, and consequently a steep slope at the origin of the variogram and a high *TBS* value. Conversely, a 2D projection of deteriorated bone architecture produces an image with a low number of pixel value variations of high amplitude, and therefore a mild slope at the origin of the variogram and a low TBS. It was found that *TBS* correlated positively with the BMD and decreased with age [6].

More studies found that trabecular bone microarchitecture showed the spatial organization and morphology of the trabecular network. Anisotropy of the trabecular bone may also be used to predict fracture risk [14]. Different methods have been used to study characterized the structure anisotropy on trabecular radiographs. A semi-quantitative index was applied to femoral neck radiographs [15]. This index is based on the presence of several arches of trabeculae in the femoral neck. Some arches preferentially disappear with age and osteoporosis, and counting of these arch systems can be used to determine that semi-quantitative index. Fractal analysis on bone radiographs was proposed [16]. The measured parameters provide a global assessment of the image irregularities as an indicator of roughness. The Maximum Likelihood Estimator is applied first on a specific direction. Then, the process is repeated in 36 directions in steps of 10 de-

grees. The orientation results can be represented by a polar diagram, which itself can fit an ellipse; the shape of the polar diagram can be characterized to determine textural anisotropy. Fast Fourier transforms (FFT) were applied to regions of interest in trabecular bone radiographs, with all FFT spectra involving horizontal and vertical components corresponding to longitudinal and transversal trabeculae respectively [10].

In current paper, the directional trabecular bone scores, TBS_x and TBS_y, along the directions perpendicular and parallel to the forearm were calculated from X-ray images of trabeculae located at the ultra-distal radius. The ratio of TBS_x and TBS_y was used to evaluate the anisotropy of the trabecular bone.

The results of current studies show that anisotropy of *TBS* has the potential to be used quantitatively to assess age-related and/or pathological changes in the microstructures of ultra-distal radius, which may influence bone fragility. If the anisotropy of *TBS* proposed in this study was applied, it can be directly evaluation quantitatively on the projection X-ray images obtained in routine clinical practice. In additional to quantifying the microstructures of ultra-distal radius as shown in current study, the anisotropy of *TBS* can also be used to quantitatively assess the microstructures of other trabecular bones. The overall purpose of such a study is to understand whether radiographically determined trabecular bone micro-architecture can improve clinicians' ability to estimate patients' risk of osteoporotic fracture, beyond that obtained using bone mass measurements alone.

5. Limitations

This study has several limitations. First, the irregular shape of the trabecular bone located at ultra-distal radius may produce uneven bone image due to thickness variations along the projection direction in clinical settings. Second, all measurements of *BMD* reported in this study were obtained from a GE Lunar Prodigy DXA scanner, so our findings can not necessarily be extrapolated to scanners from other manufacturers due to the ultra-distal radius sites of different DXA scanners. The ROI may vary slightly from scanner to scanner. Third, standardized settings for X-ray image acquisition procedures need to be developed because the image signal received by the X-ray detector depends on the energy and intensity of X-rays. This should include the development of automatic compensation techniques related to digital detector's characteristics, as well as methods to generate good reproducibility. In the current study, we only analyzed images of trabecular bone and didn't process any images of cortical bone.

6. Conclusion

The results of this study demonstrate that healthier trabecular bone located at the ultra-distal radius will have greater anisotropy. Imaging analysis of the anisotropy of trabecular bone texture may potentially play an alternative role in the

study of osteoporosis and bone health.

Conflicts of Interest

The authors declare no conflicts of interest regarding the publication of this paper.

References

[1] Shevroja, E., Lamy, O., Kohlmeir, L., Koromani, F., Rivadeneira, F., and Hans, D. (2017) Approach to Dual-Energy X-Ray Absorptiometry (DXA) for Fracture Risk Assessment in Clinical Practice. *Journal of Clinical Densitom*, **20**, 334-345. https://doi.org/10.1016/j.jocd.2017.06.019

[2] WHO Study Group (1994) Assessment of Fracture Risk and Its Application to Screening for Postmenopausal Osteoporosis. *Osteoporosis International*, **4**, 368-381. https://doi.org/10.1007/BF01622200

[3] Lin, J., Boechat, M.I., Deville, J.G., Gilsanz, D., Stiehm, R., Gilsanz, V., Salusky, I. and Nielsen-Saines, K. (2012) Quantitative Computerized Tomography (QCT) versus Dual X-Ray Absorptiometry (DXA) in the Assessment of Bone Mineral Density of HIV-1 Infected Children. *World Journal of AIDS*, **2**, 306-311. https://doi.org/10.4236/wja.2012.24041

[4] Stone, K., Seeley, D., Lui, L., Cauley, J., Ensrud, K., Browner, W., Nevitt, M. and Cummings, S. (2003) BMD at Multiple Sites and Risk of Fracture of Multiple Types: Long-Term Results from the Study of Osteoporostic Fractures. *Journal of Bone Mineral Research*, **18**, 1947-1954. https://doi.org/10.1359/jbmr.2003.18.11.1947

[5] Rice, J., Cowin, S. and Bowman, J. (2003) On the Dependence of the Elasticity and Strength of Cancellous Bone on Apparent Density. *Journal of Biomechanics*, **21**, 155-168. https://doi.org/10.1016/0021-9290(88)90008-5

[6] Pothuaud, L., Carceller, P. and Hans, D. (2008) Correlations between Grey-level Variations in 2D Projection Images (TBS) and 3D Microarchitecture: Applications in the Study of Human Trabecular Bone Microarchitecture. *Bone*, **42**, 775-787. https://doi.org/10.1016/j.bone.2007.11.018

[7] Krueger, D., Fidler, E., Libber, J., Berengere, A., Hans, D. and Binkley, N. (2014) Spine Trabecular Bone Score Subsequent to Bone Mineral Density Improves Fracture Discrimination in Women. *Journal of Clinical Densitom*, **17**, 60-65. https://doi.org/10.1016/j.jocd.2013.05.001

[8] Iki, M., Fujita, Y., Tamaki, J., Kouda, K., Yura, A., Sato, Y., Moon, J., Winzenrieth, R., *et al.* (2015) Trabecular Bone Score May Improve FRAX1 Prediction Accuracy for Major Osteoporotic Fractures in Elderly Japanese Men: The Fujiwarakyo Osteoporosis Risk in Men (FORMEN) Cohort Study. *Osteoporos International*, **26**, 1-8. https://doi.org/10.1007/s00198-015-3092-3

[9] Whitehouse, W. (1974) The Quantitative Morphology of Anisotropic Trabecular Bone. *Journal of Microscopy*, **101**, 153-168. https://doi.org/10.1111/j.1365-2818.1974.tb03878.x

[10] Brunet-Imbault, B., Lemineur, G., Chappard, C., Harba, R. and Benhamou, C. (2005) A New Anisotropy Index on Trabecular Bone Radiographic Images Using the Fast Fourier Transform. *BMC Medical Imaging*, **5**, 1-11. https://doi.org/10.1186/1471-2342-5-4

[11] Chen, J. and Ying, Q. (2022) Imaging Analysis of Trabecular Bone Texture Based on the Initial Slope of Variogram of Ultra-Distal Radius Digital X-Ray Imaging: Effects

on Bone Mineral Density and Age. *Open Journal of Radiology*, **12**, 78-85. https://doi.org/10.4236/ojrad.2022.123009

[12] Healthcare, G.E. (2010) Lunar enCORE-Based X-Ray Bone Densitometer User Manual. https://www.gehealthcare.com/-/media/20fc07d1369e4d15acae5732090559db.pdf?la=en-us

[13] Mukaka, M.M. and Corner, S. (2012) A Guide to Appropriate Use of Correlation Coefficient in Medical Research. *Malawi Medical Journal*, **24**, 69-71.

[14] Sugita, H., Oka, M., Toguchida, J., *et al.* (1999) Anisotropy of Osteoporotic Cancellous Bone. *Bone*, **24**, 513-516.

[15] Aggarwal, N.D., Singh, G.D., Aggarwal, R., Kaur, R.P. and Thapar, S.P. (1986) A Survey of Osteoporosis Using the Calcaneum as an Index. *International Orthopaedics*, **10**, 147-153. https://doi.org/10.1007/BF00267758

[16] Jiang, C., Pitt, R.E., Bertram, J.E.A. and Aneshansley, D.J. (1999) Fractal-Based Image Texture Analysis of Trabecular Bone Architecture. *Medical & Biological Engineering & Computing*, **37**, 413-418. https://doi.org/10.1007/BF02513322